

# **Ultrasonic P-wave propagation through water-filled rock joint: An experimental investigation**

Yang H.<sup>a,b</sup>, Duan H.F.<sup>a,b</sup>, Zhu J.B.<sup>c,\*</sup>

<sup>a</sup> Department of Civil and Environmental Engineering, The Hong Kong Polytechnic University, Hong Kong SAR

<sup>b</sup> Research Institute for Sustainable Urban Development, The Hong Kong Polytechnic University, Hong Kong SAR

<sup>c</sup> State Key Laboratory of Hydraulic Engineering Simulation and Safety, School of Civil Engineering, Tianjin University, Tianjin, China

\* Corresponding author, Email: [jbzhu@tju.edu.cn](mailto:jbzhu@tju.edu.cn)

**Abstract:** The presence of fluids in rock discontinuities may dramatically affect wave behaviours of rock masses, e.g., wave velocity, wave transmission and attenuation. In this study, extensive laboratory tests of ultrasonic P-wave propagation across water-filled rock joints were conducted to investigate the effects of joint thickness and water content on compressional wave propagation in the ultrasonic frequency range were investigated. P-waves with two different central frequencies of 0.1 MHz and 1.0 MHz were applied to study ultrasonic wave characteristics of rock with a single water-filled joint under different joint-thickness-wavelength-ratio conditions. The experimental data were collected and used for the analysis of wave velocity, transmission coefficient and attenuation quality factor of rock samples with water-filled rock joints. The results showed that the increase of joint thickness could cause more wave attenuation while the increase of water content could lead to less wave attenuation. In addition, the wave velocity is higher, yet wave transmission is weaker for higher-frequency waves (1MHz). The results and findings were elaborated and explained through the fundamental physics of acoustics in fluids and rocks. The present paper is of great significance to characterize the wave responses of rock discontinuities filled with fluids.

**Keywords:** Ultrasonic wave; water-filled rock joint; wave velocity; wave attenuation

## 1. Introduction

Rock joints universally exist in nature and highly affect wave propagation and attenuation in rock masses (King et al., 1986). Natural joints can be unfilled or filled with various materials, e.g., calcite, anhydrites, chlorite, phyllosilicates, gypsum, quartz sand, clay, water, gas and oil (Morrow et al., 1994, Ague, 1995, Jaeger et al., 2009, Aydin, 2000, Morad et al., 2010, Trippetta et al., 2010, Carminati et al., 2014, Lipparini et al., 2018). Understanding the interaction of wave propagation and rock joints is of great significance to geophysical exploration and surveying, earthquake engineering, rock mechanics as well as non-destructive evaluation.

Considerable studies have been conducted to investigate influences of the non-filled rock joints on wave behaviours in rock masses. Pyrak-Nolte et al. (1990) conducted experimental and analytical studies on wave propagation across single natural rock joints, and they defined the joint specific stiffness for better interrelating mechanical and seismic behaviours of rock joints. Zhao and Cai (2001) and Zhao et al. (2006) analytically studied wave propagation through single linear and non-linear rock joints. Thereafter, Zhao et al. (2006a) and Zhao et al. (2006b) investigated effects of multiple parallel rock joints on wave behaviours. Recently, Zhu et al. (2011) and Zhu and Zhao (2013) analytically studied normally and obliquely incident wave propagation across a joint set with the virtual wave source method (VWSM). In these studies, the displacement discontinuity method (DDM) was adopted to obtain mathematical solutions of wave propagation across rock joints. In the DDM, the non-filled joint is commonly treated as a non-weld interface, across which stresses are continuous while displacements are discontinuous (Schoenberg, 1980).

Regarding the filled rock joints, some laboratory studies have been performed on joints filled with granular materials, and found that properties of filling materials (e.g., water content, particle size and composition), joint thickness, loading rate and input energy strongly affected stress wave propagation through filled rock joints (Li and Ma, 2009, Wu et al., 2014, Wu and Zhao, 2015). On the other hand, analytical work found that the DDM was only valid for filled joints with the thickness much smaller than the wavelength of the incident wave (Li et al., 2010, Ma et al., 2011). To this end, another analysis approach - the layered medium method (LMM) was developed since the LMM is applicable for the analysis of wave propagation across joints regardless of the ratio of joint thickness to the wavelength. In the LLM, the joint was regarded as a layer sandwiched between two solids, and both stresses and displacements are treated to

be continuous across the two interfaces between the layer and background half-spaces (Brekhovskikh, 1980, Rokhlin and Wang, 1991). Combined the LMM with Kelvin and Maxwell models, Zhu et al. (2011) derived analytical solutions for wave propagation through a single viscoelastic filled joint. Using the modified recursive method, wave transmission and reflection through multiple parallel filled rock joints were analytically studied by Zhu et al. (2012). Recently, Li et al. (2013) and Li et al. (2014) developed the thin-interface model to study stress wave normally and obliquely propagating through a filled joint.

In addition to rock joints filled with granular materials, fluid-filled rock joints also widely exist in Earth's crust. Applications of acoustic waves for detecting and characterising fluid-filled rock joints have become more and more common and popular in many fields, such as mining engineering, petroleum engineering, geothermal engineering, engineering geology, and hydrology, etc. (Xu and Parra, 2003, Risnes et al., 2005, Davatzes and Hickman, 2010, David et al., 2015, Montone and Mariucci, 2015 Nicolas et al., 2016, Trippetta and Geremia, 2019). Therefore, it is necessary and significant to understand and inspect wave behaviours and responses to fluid-filled rock joints. However, few studies have been done to investigate wave propagation across fluid-filled rock joints. Fehler (1982) obtained analytical transmission and reflection coefficients for waves (including P, SV and SH waves) propagating through a viscous fluid layer at arbitrary incident angles based on the LMM. Pyrak-Nolte et al. (1990) experimentally investigated the presence of fluid in single rock joints on wave propagation across joints. However, they merely studied a fracture with quite small thickness (largest aperture of 0.1 mm) compared with the wavelength (about 10 mm). In addition, among above literatures, the quantification of effects of properties of fluid-filled joints on wave behaviours were sparsely documented.

This paper presents an experimental study on the wave responses to water-filled rock joints, aiming to further understand the interaction between P-wave propagation and single water-filled rock joint. Firstly, a series of ultrasonic tests were conducted in the laboratory for the water-filled rock joints to quantify the impacts of the joint thickness and the filling water volume content in the joint on P-wave responses (velocity and energy). Incident waves with two different frequencies, i.e., 0.1 MHz and 1.0 MHz, were tested to study the differences in wave responses to different ratio of rock joint thickness to the wavelength. Subsequently, acoustic properties, i.e., the specific wave velocity, transmission coefficient as well as attenuation quality factor, of the single water-filled rock joint were evaluated and analysed. With extensive experimental data analysis, the physical mechanisms lying behind were

discussed in detail from a viewpoint of acoustics in fluids and wave propagation through layered media. The results and findings from this study may serve as a useful guide for the interpretation of field measurements, as well as can contribute to better understanding wave behaviours of fluid-filled rock joints.

## **2. Experimental methodology**

### **2.1 Sample preparation**

Granite rock from Hunan province, mainland China, was selected to prepare samples for this study. The mineralogical composition of the granite rock consists of quartz (39.3%), plagioclase (17.9%), microcline (21.4), biotite (19%) and chlorite (2.4%), as shown in Fig. 1c. And grain size of the rock ranges from 0.1 to 2.0 mm. An intact rock sample and a jointed one were manufactured from the same granite rock core, as shown in Fig. 1a. The end surfaces of rock samples were flat and parallel to ensure good contact between the rock sample and transducers. The size of these rock samples is 49 mm in diameter and 100 mm in length. A single natural joint is located at the midplane of the jointed rock sample, and approximately orthogonal to its axial direction. The three-dimensional joint roughness coefficient (JRC) of the natural joint was evaluated to be approximately 9.65 with the aid of the digital surface scanner (Yang et al., 2001, Li et al., 2018), as shown in Fig. 1a. It is also noted the two surfaces of the natural joint partially contacted with each other, that is, the natural joint has a low matedness. This intact rock sample could be used to obtain reference wave data for analysing wave behaviours and responses to rock joints (Pyrak-Nolte et al., 1990; Huang et al., 2014). Other essential mechanical and physical properties of these two rock samples were determined with standard rock mechanics laboratory tests (ISRM, 1979, ASTM Designation D3148-72) and listed in Table 1. These two rock samples were immersed in water under a vacuum pressure of 0.8 kPa for 24 hours prior to the ultrasonic tests, with the aim to eliminate the influence of local fluid flow in microcracks and pores on wave propagation in rock samples.

The jointed rock sample was used to artificially produce a series of water-filled rock joints. In details, a prepared heat-shrinkable tube with an inner diameter of 49 mm and a length of 30 mm was firstly used to wrap the original natural rock joint. The waterproof tape was used to hold rock bodies and the tube together, as shown in Fig. 1b. Both of heat-shrinkable tube and sealing tape could avoid the leakage of filling water. Thereafter, two halves of the jointed rock sample were separated along its central axis at a certain distance. The distance between two halves of the jointed rock sample was measured by a Vernier calliper with a precision of 0.01

millimetre, which was termed as the joint aperture in this study. As a result, an open joint with a fixed joint thickness was generated. Note that the volume of this open joint was determined approximately by measuring the total volume of filled water injected in the joint. According to the obtained total volume of the open joint, various air-water filled joints could be produced by injecting water at different volumes into the joint. There were two small holes at the highest side edge of the tube, with one for injecting water and the other for releasing the air in the joint during injection. Therefore, when water was injected to the open joint, inside pressure of the open joint kept stable at atmospheric pressure and had negligible effects on rock bodies. Following above process, water-filled rock joints with different joint thicknesses and various filling water contents were established for ultrasonic tests. Different from these artificial water-filled rock joints, the natural joint under the original matching condition was regarded as a closed joint. It is necessary to point out that in this study the dry closed joint refers to joint with only air existing in apertures between two joint surfaces. In contrast, the wet closed joint means that apertures between two joint surfaces are fully filled with water.

## 2.2 Experimental apparatuses

The ultrasonic pulse transmission technique, one of the commonly used non-destructive methods (Brich, 1960, Kern, 1982, Pyrak-Nolte et al., 1990, Cadoret et al., 1995), was applied in this study to experimentally investigate ultrasonic wave propagation in rock masses with single fluid-filled rock joints. As shown in Fig. 2, the ultrasonic testing system consists of a pair of Olympus P-wave transducers, an Olympus pulser/receiver (model 5077PR), a Tektronix digital oscilloscope (DPO 2012B) and a PC for data acquisition. Rock samples were sandwiched between two transducers with good connection by applying Vaseline to the interface. To make better coupling between rock end surfaces and transducers, a low uniaxial pre-pressure of 0.01 MPa was applied to the assembly of transducers and the rock sample. The jointed sample was fixed using two steel callipers before loading in case of unexpected deformation of the joint. During the tests, however, this relatively low pressure was maintained only for around 1 minute for interface coupling, so that the loading and the fixing device would be removed before ultrasonic measurements.

The transmitter (the transducer emitting input signals) was pulsed by a 400-V spike with a duration of 10  $\mu$ s at a repetition rate of 100 Hz to produce compressional waves while the receiver (the transducer receiving ultrasonic waves) was used to detect the transmitted pulses through rock samples. Two pairs of transducers with different central frequencies, i.e., model X1020 (0.1 MHz) and model V192 (1.0 MHz), were used in this study. In addition to generating

signals, the pulser/receiver connected to transducers could also receive the transmitted signals with connecting the digital oscilloscope. The oscilloscope was used to digitize, display and record a portion of each ultrasonic signal with duration of 100  $\mu$ s. The sampling interval of this oscilloscope was 0.001 $\mu$ s. To maximize the signal-to-noise ratio and to obtain stable waveforms, 256 signals were stacked and averaged for each measurement. A PC equipped with data acquisition software was connected to the oscilloscope to store experimental data. The delay time and precision of this ultrasonic system were  $1.125 \pm 0.111 \mu$ s and  $0.423 \pm 0.040 \mu$ s for P-wave transducers of 0.1 MHz and 1.0 MHz, respectively, which were determined by directly docking the transmitter to the receiver.

### 2.3 Experimental scheme

To calibrate the testing system and measurement facilities, ultrasonic tests on the dry and wet closed joints were firstly conducted. In addition, ultrasonic signals of the intact rock sample were measured to obtain the reference data (Pyrak-Nolte et al., 1990). Following that, water-filled rock joints with five water filling degrees, i.e., 0%, 25%, 50%, 75% and 100%, and seven joint thicknesses, i.e., from 2 mm to 14 mm with an interval of 2 mm, were tested to quantitatively investigate effects of the water volume content in the joint and the joint thickness on wave behaviours. The generation of all artificially open joints with varied joint thicknesses was achieved by separating two halves of the jointed sample at a certain distance by the tester. Herein, water content in the joint refers to the percentage of filled water volume to the whole volume of the joint aperture. And the changing water content in the joint were achieved by injecting water of different volume using a syringe. In total, 38 sample scenarios were tested (No. 1 for intact sample without joint, No. 2 for closed joints with approximately zero thickness, and the rest 35 cases for open water-filled joints with different thicknesses). Two types of P-waves, i.e., Type I with frequency of 0.1 MHz and Type II with frequency of 1.0 MHz, were applied in this study to explore wave responses to different joint thickness-wavelength ratios. Moreover, each testing scenario was repeatedly measured for five times at similar room temperature ( $20 \pm 1^\circ\text{C}$ ) to obtain the average values and standard deviations as well as to reduce the possible system noises and operation errors that are usually inevitable in practice during the tests. Therefore, a total of 380 measurements were performed in this study.

### 3. Results and Analysis

#### 3.1 The received transmitted waveforms

Transmitted signals in the time domain were collected from the testing system and used to determine the wave responses of rock with a single water-filled joint. Typical transmitted waveforms for the input ultrasonic P-wave frequencies of 0.1 MHz and 1.0 MHz are illustrated in Fig.3. Based on these measured signals, ultrasonic wave propagation through a single rock joint filled with water can be further analysed. It is observed from Fig.3 that:

- (1) The travel time increased with decreasing water content in the joint or increasing joint thickness;
- (2) the amplitude of the wave signals increased with increasing water content in the joint or decreasing joint thickness;
- (3) the wave amplitude increased much more significantly when water content in the joint was doubled at a given joint thickness than joint thickness was halved at a certain water content;
- (4) the wave travel time increased greatly while the wave amplitude decreased slightly with increasing joint thickness at a given water content;
- (5) the wave travel time increased slightly while the wave amplitude decreased greatly with reducing water content at a certain joint thickness.

#### 3.2 Wave velocity

As one of the most important acoustic properties, wave velocity in jointed rock masses is strongly affected by joint properties, such as joint roughness, properties of filling materials and orientation of joints (King et al., 1994, Kahraman, 2002). In the literature, the wave velocity in the rock sample usually refers to the time-averaged velocity, which is the ratio of the total length of the rock sample to the travel time of main wave propagation through the rock sample, as suggested by the ASTM standard (2008). The mean values and standard deviations of wave velocity for the water-filled jointed rock samples under different test conditions were calculated and listed in Table 2. Herein, to better characterize the effects of joint thickness and water content in the joint on the wave velocity, the decrease rate of the wave velocity (DRV) was adopted (El Azhari and El Hassani, 2013)



$$DRV = \frac{V_{P\_intact} - V_P}{V_{P\_intact}} \times 100\% \quad (1)$$

where  $V_{P\_intact}$  was the measured wave velocity of the intact rock sample, and  $V_P$  was the wave velocity of a jointed rock sample.

Fig. 4 shows the DRV for ultrasonic wave propagation across a single water-filled rock joint for different joint thickness and water content in the joint. It is shown that the DRV linearly and significantly increased with increasing joint thickness, indicating that the average wave velocity through the jointed rock sample decreased considerably with the increase of joint thickness at a given water filling level. Similar findings were observed for rock joints filled with gouge (Tanimoto, C. and Kishida, K., 1994, Fratta, D. and Santamarina, J.C., 2002). This is mainly because the wave velocity of the whole jointed sample is the weighted average of the relatively higher wave velocity in the rock matrix and the relatively lower wave velocity in the infilling fluids. Consequently, an increase of joint thickness gives rise to decreasing wave velocity through the whole jointed rock sample. By contrast, with the increase of water content in the joint, the DRV decreased slightly with increasing water content in the joint. This result implies that higher water content results in faster wave velocity of the jointed rock sample. Considering the wave velocity in water is higher than that in air, the increase of water content leads to higher wave velocity in the water-filled joint, causing an increase in the averaged wave velocity in the whole jointed rock. It was observed that the wave velocity of the whole jointed rock was more sensitive to the change of the joint thickness compared with the filled water content in the joint.

In this study, to further quantify the influence of the water-filled joints on wave propagation, acoustic wave velocity through the water-filled rock joint only was also evaluated and investigated

$$V_{WP} = \frac{H}{t - t_0} \quad (2)$$

where  $V_{WP}$  is the wave velocity through the water-filled joint;  $H$  is the joint thickness;  $t$  and  $t_0$  represent the measured arrival time of the transmitted pulse through the jointed rock sample and the reference intact rock sample, respectively. The term  $t - t_0$  refers to the travel time of main wave through the water-filled rock joint.

The calculated mean values and standard variations of wave velocity through the water-filled joints are listed in Table 3. It showed that higher water content in the joint could cause higher wave velocity across the water-filled joint, which was mainly due to the relatively high wave velocity in water than in air. On the other hand, it was found that with increasing joint thickness, the average wave velocity through the water-filled joint increased before roughly keeping constant. This is caused by the variation in volume fraction of entrained air in water filled in the joint. That is, a small amount of air could be entrained when sucking up water into a syringe, which would be introduced into the open joint during water injection. As a result, the very small fraction of air entrained in water would significantly reduce wave speed in water (Wylie et al., 1993). With the increase of joint thickness, the volume fraction of entrained air relative to the total volume of infilling water gradually decreased to a constant value, so the resulted wave speed in filling water slightly increased, thereby increasing wave velocity in the water-filled joint.

In addition, the DRV might change with rock type, since the properties of host rock have substantially contributed to the overall wave velocity. In this study, we mainly focused on such DRV varying with the properties/parameters of filled fluid in joints. And hence, host rock types were not studied.

### 3.3 Frequency spectra

The frequency spectra are important to reveal wave information (modification and shift) in the frequency domain, which could be calculated by the fast Fourier transform (FFT) technique. The received wave is composed of the initial pulse and the subsequent ones from reflections at various interfaces such as contact interfaces between the sample and transducers. Therefore, it is necessary to extract initial pulses from complete waveforms. For this reason, an appropriate window function should be selected to taper the received signals, which has very few effects on spectra of original signals and preserve more low-frequency contents without too much distortion in high-frequency range (Pyrak-Nolte et al., 1990). Tapering is a process to extract a specific pulse of finite duration from a complete signal by multiplying the complete signal with the window function. After trials and errors, to extract the initial pulses for the spectral analysis in this study, a half-cosine taper with a 9- $\mu$ s window function (see Fig. 5a) was applied to the received signals from the ultrasonic transducer of 0.1 MHz while a half-cosine taper with a 5- $\mu$ s window (see Fig. 5b) was applied to the received signals from the ultrasonic transducer of 1.0 MHz. Amplitudes of these two tapers both equal to unity. Thereafter, the FFT was applied to obtain corresponding amplitude spectra in the frequency domain.

Figs. 6 and 7 showed that the mean values and standard deviations of the spectral amplitudes for different joint thicknesses and water content in the joint, where the incident wave frequencies are 0.1 MHz and 1.0 MHz, respectively. Herein, to validate the testing system and measurement facilities, ultrasonic tests on the dry and wet closed joints (i.e., joint thickness is regarded as 0 mm compared with the other macro-scale joint apertures in this study) were first conducted and analysed. Spectra for transmitted waves through dry and wet closed joints (Figs. 6a and 7a) implied that spectral amplitudes for wet closed joint were much higher than those for the dry closed joint, which was in accordance with previous findings (Pyrak-Nolte et al., 1990) and thus verified the applicability testing system used in this paper. It could be attributed to that the presence of water could increase the joint specific stiffness due to higher bulk modulus of water compared to air, resulting in more wave energy transmission through joints (Pyrak-Nolte et al., 1990).

Figs. 6 and 7 also demonstrated that, in comparison with intact rock sample, the wave spectral amplitudes for jointed rock samples were greatly attenuated. More specifically, the amplitude of transmitted wave through a water-filled rock joint was one order lower than that through the intact rock. In addition, it was found that the extent of wave spectral amplitude attenuation decreased with increasing water filling degree. For example, with the water content increasing from 25% to 100%, the transmitted wave amplitude increased by approximately one order. One possible explanation for this was that the increase of water content in the joint resulted in higher bulk modulus of the joint and then caused larger joint specific stiffness, thereby enhancing wave transmission. Besides, larger area of the water-rock interface caused by higher water content in the joint led to less wave reflection. Despite of the dependence of wave spectra amplitude on water content, the uncertainty of the testing results, i.e., the standard deviation bars on the curves in Figs. 6 and 7, also increased due to the increasing wave energy transmissions during the testing process. An obvious shift of the central frequencies, i.e., frequencies corresponding to maximum spectral amplitudes, of transmitted waves through the water-filled joint could be observed by referring to the incident P-wave frequencies. And the shifting effect was more significant for waves with relatively high frequency (e.g., P-wave Type II with a frequency of 1.0 MHz).

### 3.4 Wave transmission coefficient

Wave transmission coefficient is an essential factor to characterize wave attenuation through the rock joint. The transmission coefficient for elastic wave on the interface was defined as (Rokhlin and Huang, 1992, Nakagawa et al., 2000)

$$T_{ct} = \frac{A_{2\_max}(t)}{A_{1\_max}(t)} \quad or \quad T_{cf} = \frac{A_{2\_max}(f)}{A_{1\_max}(f)} \quad (3)$$

where  $T_{ct}$  and  $T_{cf}$  denotes the transmission coefficient in the time domain and frequency domain, respectively;  $A_{1\_max}(t)$  and  $A_{2\_max}(t)$  refer to maximum voltages of received initial signals through the intact and jointed rock samples respectively in this study, and  $A_{1\_max}(f)$  and  $A_{2\_max}(f)$  represent the maximum spectral amplitudes of tapered initial waves across the reference intact and the jointed samples, respectively.

Fig. 8 showed transmission coefficients in both time and frequency domains for ultrasonic P-wave transmission across a single water-filled rock joint with different water contents in joints, where the wave frequencies are 0.1 MHz and 1.0 MHz. Testing results in time domain showed that the wave transmission coefficient decreased with increasing joint thickness, which is accordance with analytical results predicted by the layered medium model (Zhu et al., 2012). For example, at a water content of 100%, the transmission coefficient decreased by about 25% when the joint thickness increased from 2 mm to 14 mm. The explanation is that larger joint thickness could lead to longer propagation path, thereby causing more energy dissipation in the water-filled joint. The wave transmission coefficient increased significantly with the increase of water content in the joint. For instance, it increased by over 5 times when the water content increased from 25% to 100% and joint thickness was 14mm. This is because that the increase of the water content gave rise to a larger area of the water-rock interface, leading to less wave reflection at joints since the water-rock impedance mismatch was smaller than air-rock one. In addition, increasing water content could result in more wave energy transmission across the joint since energy loss in water is smaller than that in air part.

Testing results in the frequency domain showed the similar trends to those in the time domain, as shown in Fig. 8. However, the influence of joint thickness in the frequency domain was less significant than that in the frequency domain, in comparison with that variation trend in the time domain. This is mainly due to the frequency shifting effects during wave transmission, as shown in Figs. 6 and 7, which results in the energy re-distribution and averaging among different harmonic modes in the frequency domain. Besides, it was observed that the calculated transmission coefficient in the frequency domain was slightly smaller than that in the time domain. A possible explanation is that the frequency-domain transmission coefficient is determined by the amplitude of the dominant mode among all decomposing harmonic waves coming from time-domain initial transmitted signals. It was also found that transmission

coefficients for 0.1-MHz waves were larger than those for 1.0-MHz, which indicated that more wave transmitted across the water-filled rock joint for the incident wave at lower frequency.

### 3.5 Wave attenuation quality factor $Q$

The attenuation quality factor  $Q$  is commonly used to characterize wave attenuation in rock materials. The spectral ratio method (Toksöz et al., 1979; Johnston and Toksöz, 1980; Sears and Bonner, 1981) has been widely used to determine the quality factor  $Q$  by comparing the waveform spectra propagating through rock samples with those through a reference specimen with negligible attenuation. On this basis, the quality factor of the jointed rock specimen can be expressed by (Toksöz et al., 1979),

$$\ln \frac{1}{2} = \left( \frac{1}{2} \frac{1}{1} \right) \frac{\pi}{\lambda} + \ln \frac{1}{2} \quad (4)$$

where  $\omega$  is the wave frequency;  $A_1$  and  $A_2$  are the spectral amplitudes obtained by conducting FFT on tapered initial transmitted pulses through the reference sample and the jointed rock sample, respectively;  $v_1$  and  $v_2$  refer to the phase wave velocities of the reference sample and the jointed rock sample, respectively;  $Q_1$  and  $Q_2$  denote quality factors of the reference sample and the jointed rock sample, respectively;  $L$  is the traveling path length;  $G_1$  and  $G_2$  stand for the geometrical factors for the reference sample and the jointed rock sample, respectively. In this study, seven aluminium samples were prepared to obtain reference data for calculating quality factors of different jointed samples, because the aluminium material could be regarded non-dissipative compared with rock materials. It is assumed that the quality factor of aluminium sample is much higher than that of jointed rock sample. Therefore,  $Q_1$  is assumed to be infinite in this paper. As a result,  $Q_2$  of the jointed rock sample can be given by

$$\frac{1}{Q_2} = \frac{\pi}{2} \frac{L}{\lambda} + \frac{1}{Q_1} \quad (5)$$

Note that for simplicity,  $Q$  is used to represent  $Q_2$  in the following analysis. Due to the same size between the reference aluminium and jointed rock samples, the effect of constant geometric factor, i.e.,  $G_1 / G_2$ , is negligible when calculating  $Q$ . The calculated quality factor showed wave attenuation of rock samples containing a single fluid-filled joint. Eq. (5) indicates that a smaller  $Q$  means more significant wave attenuation.

Fig. 9 showed  $Q$  as a function of joint thickness for different water content in the joint where the frequencies of incident waves are equal to 0.1 MHz and 1.0 MHz, respectively. And the standard variations of  $Q$  values for different jointed rock samples were given in Table. 4. It was

found that  $Q$  decreased as the joint thickness increases. For example,  $Q$  for 0.1-MHz wave reduced by 2.4% when joint thickness increases from 4 mm to 6 mm for a given water content of 50%. It was also observed that the increase of water content in the joint significantly increased  $Q$ . Specifically,  $Q$  for 0.1-MHz wave increased by about 6.7% when water content increased from 50% to 75% for a certain joint thickness of 6 mm. These observations showed that water content in the joint had more significant influence on values of  $Q$  compared with joint thickness. Based on these  $Q$  values, it was found that wave attenuation in water-filled jointed sample increased with the increasing joint thickness. This could be attributed to the fact that the longer water-filled joint could cause more wave energy loss due to the increasing travelling path in the joint. Besides, increasing water content in the joint could result in less wave attenuation. It could be explained by that, for the fluid layer sandwiched by two halves of rock matrix, the area of water-solid interface increased with increasing water content, thereby causing much more energy transmitted into fluid-filled joint (Stein and Wysession, 2009). Moreover, increasing water content led to the higher bulk modulus of filling water-air layer. Consequently, joint specific stiffness increased, which caused more wave energy transmission (Zhu et al., 2012). In addition, wave motion in fluids filled in the joint also made wave energy lost, which was described in detail in next section in terms of acoustics in fluids. Fig. 9 also revealed that  $Q$  values for the 0.1-MHz incident wave was smaller than those for the 1-MHz incident wave. One possible explanation is that more wave energy was concentrated in the selected frequency range for calculation of  $Q$  for 1-MHz wave compared with 0.1-MHz one.

#### 4. Discussion

Above experimental results and analysis have shown that the joint thickness and filled water content could significantly affect wave propagation, attenuation and slowness. The physical mechanisms lying behind can be further explained by the classic acoustics in fluids. As shown in Fig. 1b, the artificial water-filled joint with the soft covering tube could be regarded as a symmetric water-filled pipe column, in which the fundamental frequency can be determined theoretically by  $v_p/2L$ , with  $v_p$  being wave speed and  $L$  the length of water-filled pipe column (Lee et al., 2006). With the increase of joint thickness, i.e., greater  $L$ , the fundamental frequency of the joint decreases. According to the fundamental acoustics in fluid mechanics (Louati and Ghidaoui, 2017a, Che et al., 2018), as the high-frequency wave propagates in the water-filled



pipe, there would be less high-frequency modes occurring in the relatively lower frequency system due to the relatively low group velocity of wave dispersion along the fluid-filled pipeline. Note that the incident P-wave frequencies in this study are much higher than the cut-off frequencies of the water-filled joints for all tests. As a result, the influence of joint thickness on the wave propagation speed in the water-filled rock joint could be obtained as shown in Table 3. On the other hand, with regard to the influence of filled water content, the wave propagation velocity is much higher in the water than in the air according to the basic fluid mechanics and physics (Chaudhry, 2014). For air-water mixture, the wave velocity is mainly affected by the weighted volumes of both the water and air (Wood, 1949). As a result, the average wave velocity becomes higher when the water content is larger, which is consistent with the results listed in Table 3.

Regarding wave attenuation caused by the water-filled rock joint, increasing joint thickness could result in more high-frequency components of transmitted P-wave through the water-filled rock joint (Louati and Ghidaoui, 2017b). Therefore, more energy loss due to the fluid viscous effect was caused when these high-frequency waves travelled a longer path in the water-filled joint, as observed in Figs. 8 and 9 in this study. Furthermore, the effects of filled water content in joints on wave transmission and attenuation could be partly attributed to the changes of the compressibility (density) and viscosity of the mixed air-water media with different weights of water and air in the joint (Domenico, 1974). Specifically, based on the previous findings regarding fluid-wave interaction (Louati and Ghidaoui, 2017b), the fluid viscosity in the joint may have considerable influences on the high-frequency wave modes than on the low-frequency ones because of the more likely multi-path propagation of high modes in the joint. On this point, it was reasonable and understandable for the observations shown in Figs. 8 and 9.

Experimental observations in this study have also showed obvious differences in wave properties of water-filled rock joints for incident waves at different central frequencies. To demonstrate and quantify these dissimilarities, the corresponding wave responses were extracted from the testing data and illustrated in Fig. 10. Despite similar variation trends of wave velocity with joint thickness and water content in the joint, a clear increase of wave velocity with the incident wave frequency was observed from Fig. 10. The difference of wave speeds between two P-waves with different frequencies, i.e., 0.1 MHz and 1 MHz, decreased with increasing joint thickness but kept almost constant with varying filled water content. In other words, ultrasonic compressional wave velocity was more sensitive to the joint thickness

1 than to the water content. This can be explained again through the fundamental acoustics of  
2 high frequency waves in fluid systems (Rienstra and Hirschberg , 2004). Specifically, wave  
3 propagation velocities are generally higher for shorter wavelengths since they tend to find fast  
4 paths and diffract around the heterogeneities (Louati and Ghidaoui, 2017a). Moreover, the local  
5 fluid flow theory revealed that wave velocities of P-waves may increase with the wave  
6 frequency, because the water could not relax immediately which causes stiffer bulk and larger  
7 shear effects at high-frequency modes (Mavko and Jizba, 1991, Mavko and Nolen-Hoeksema,  
8 1994, Dvorkin, Mavko and Nur, 1995). In addition, our results implied that the wave  
9 transmission coefficient became relatively lower for ultrasonic waves with high frequencies.  
10 This phenomenon may be explained by the high-frequency wave filtering process from the  
11 fluid-filled joints (Pyrak-Nolte et al., 1990). That is, it was more difficult for the waves with  
12 higher frequency modes to pass through the fluid-filled joint, leading to less wave transmission  
13 and thus more wave attenuation (Müller et al., 2010).

14 This study was focused on ultrasonic wave propagation through water-filled rock joint, which  
15 is one of important geological structures in rock, especially for shallow rock. The wavelength  
16 of the ultrasonic P wave used in the study is at the scale of mm and cm. In nature, the thickness  
17 of rock joints is usually at a scale of cm or smaller, which is coincident with the joint thickness  
18 adopted in this study (Barton 1974; Sinha and Singh 2000; Zhu et al. 2012). One key parameter  
19 to affect wave propagation across rock discontinuities is the ratio between joint thickness and  
20 wavelength. According to dimensionless analysis, the findings in this study could be upscaled  
21 to wave propagation across faults, if the ratio of fault thickness to wavelength is comparable to  
22 the ratio of joint thickness to wave length in this paper. For example, 200-Hz seismic wave  
23 propagation across a fault with thickness of 1 m approximately corresponds to the case of 0.1-  
24 MHz ultrasonic wave propagation though the joint of about 2 mm thick.

25  
26 The findings in this study can serve as a guide to physically interpret the acoustic measurements  
27 in geotechnical field tests, which may include: (1) indicating the presence of in situ fluid-filled  
28 joints and providing information of their characteristics (i.e., joint aperture and fluid filling  
29 content); (2) identifying fluid-filled fractures around the borehole. In addition, this study  
30 compensates for laboratory investigations on acoustic wave propagation through large-scale  
31 fluid-filled rock joints, which enhances understanding of acoustic wave motion through fluid-  
32 filled rock discontinuities, especially for macroscopic rock joints compared with wavelengths.  
33 Since wave attenuation in rock joints is much more significant than that in rock matrix (King



et al. 1986; Pyrak-Nolte et al. 1990), we believe that the findings in this paper could be extended to the other rock materials. Though, filling fluids, air and water, are common filling materials in rock discontinuities, cases considered in this study and corresponding findings cannot cover all practical scenarios, more investigations on joints filled by other fluids, e.g., gases and oils, would be conducted in the future work. In addition, other influence factors for wave behaviours, such as environmental temperature, pressure state, joint orientation, and fluid distribution in the joint, are also necessary to be studied. Since wave data from field tests are usually utilized to decipher the lithology information (Miller and Stewart, 1990), further investigations are necessary for examining the effect of rock lithology on wave propagation across fluid-filled joints.

## **5. Conclusions**

In this study, effects of water-filled rock joints on wave propagation and attenuation in rocks have been experimentally investigated. Main conclusions of this study are summarized as follows:

- 1) The acoustic compressional wave velocity of the water-filled rock joint could be highly influenced by the joint thickness and the filled water content in the joint. Specifically, the wave velocity in the joint increases with the filled water content but decreases with the joint thickness for all the P-waves with different central frequencies used for this investigation. This is mainly due to the impacts of fluid (air and/or water) on the propagation mechanism of high-frequency waves.
- 2) The wave transmission throughout the water-filled joint increases with the filled water content and slightly decreases with the joint thickness. These results could be explained and confirmed by the difference of wave reflection at the air-rock and water-rock interfaces, as well as by the mechanism and pattern of the multi-path propagation and viscous dissipation of the high frequency modes in the fluids (air and/or water).
- 3) The different P-wave responses of 0.1 MHz and 1.0 MHz on the water-filled rock joint have been observed for all the tests. That is, for incident P-wave at higher central frequency, the wave velocity is higher, but the wave transmission is smaller.

## Acknowledgements:

This research is financially supported by National Key R&D Program of China (No.2018YFC0407002), the Hong Kong Research Grants Council (No. 25200616 and No. 15201017) and the Research Institute for Sustainable Urban Development of the Hong Kong Polytechnic University.

## References

- AGUE, J.J., 1995. Deep crustal growth of quartz, kyanite and garnet into large-aperture, fluid-filled fractures, north-eastern Connecticut, USA. *Journal of Metamorphic Geology*, 13, 299-314.
- ASTM, 2008. Standard test method for laboratory determination of pulse velocities and ultrasonic elastic constants of rock. American Society for Testing and Materials.
- ASTM Designation D3148-72. Standard Test Method for Elastic Moduli of Intact Rock Core Specimens in Uniaxial Compression. American Society for Testing and Materials.
- AYDIN, A., 2000. Fractures, faults, and hydrocarbon entrapment, migration and flow. *Marine and petroleum geology*, 17, 797-814.
- BARTON, N., 1974. A review of the shear strength of filled discontinuities in rock. Norwegian Geotech. Inst. Publ., 105, 1-38.D3148-72.
- BREKHOVSKIKH, L. M. 1980. *Waves in layered media*, Elsevier.
- BIRCH, F., 1960. The velocity of compressional waves in rocks to 10 kilobars: 1. *Journal of Geophysical Research*, 65(4), 1083-1102.
- CADORET, T., MARION, D. & ZINSZNER, B. 1995. Influence of frequency and fluid distribution on elastic wave velocities in partially saturated limestones. *Journal of Geophysical Research: Solid Earth*, 100, 9789-9803.
- CARMINATI, E., ALDEGA, L., TRIPPETTA, F., SHABAN, A., NARIMANI, H. & SHERKATI, S., 2014. Control of folding and faulting on fracturing in the Zagros (Iran): The Kuh-e-Sarbalesh anticline. *Journal of Asian Earth Sciences*, 79, 400-414.
- CHAUDHRY, M. H. 2014. *Applied hydraulic transients*. Springer.
- CHE, T.C., DUAN, H.F., LEE, P.J., MENICONI, S., PAN, B. & BRUNONE, B. 2018. Radial pressure wave behaviour in transient laminar pipe flows under different flow perturbations. *Journal of Fluids Engineering*, 140(10), p.101203.
- DAVATZES, N. C. & HICKMAN, S. H. 2010. Stress, fracture, and fluid-flow analysis using acoustic and electrical image logs in hot fractured granites of the Coso geothermal field, California, USA.
- DAVID, C., DAUTRIAT, J., SAROUT, J., DELLE PIANE, C., MENÉNDEZ, B., MACAULT, R. & BERTAULD, D., 2015. Mechanical instability induced by water weakening in laboratory fluid injection tests. *Journal of Geophysical Research: Solid Earth*, 120, 4171-4188.
- DESAI, C. S., ZAMAN, M. M., LIGHTNER, J. G. & SIRIWARDANE, H. J. 1984. Thin-layer element for interfaces and joints. *International Journal for Numerical and Analytical Methods in Geomechanics*, 8, 19-43.
- DOMENICO, S., 1974. Effect of water saturation on seismic reflectivity of sand reservoirs encased in shale. *Geophysics*, 39(6), 759-769.
- DVORKIN, J., MAVKO, G. & NUR, A., 1995. Squirt flow in fully saturated rocks. *Geophysics*, 60(1), pp.97-107.
- EL AZHARI, H. & EL HASSANI, I. E. E. A. 2013. Effect of the number and orientation of fractures on the P-wave velocity diminution: application on the building stones of the Rabat Area (Morocco). *Geomaterials*, 3, 71.

- 1 FEHLER, M. 1982. Interaction of seismic waves with a viscous liquid layer. *Bulletin of the Seismological*  
2 *Society of America*, 72, 55-72.
- 3 FRATTA, D. & SANTAMARINA, J.C., 2002. Shear wave propagation in jointed rock: State of stress.  
4 *Géotechnique*, 52(7), pp.495-505.
- 5 HUANG, X., QI, S., GUO, S. AND DONG, W., 2014. Experimental study of ultrasonic waves propagating  
6 through a rock mass with a single joint and multiple parallel joints. *Rock mechanics and rock*  
7 *engineering*, 47(2), pp.549-559.
- 8 ISRM, 1979. Suggested method for determining water content, porosity, density, absorption and  
9 related properties and swelling and slake durability index properties. *Int J Rock Mech Min Sci*  
10 *Geomech Abstr*, 16, 141-156.
- 11 JAEGER, J. C., COOK, N. G. & ZIMMERMAN, R. 2009. *Fundamentals of rock mechanics*, John Wiley &  
12 Sons.
- 13 JOHNSTON, D. H. & TOKSÖZ, M. N. 1980. Ultrasonic P and S wave attenuation in dry and saturated  
14 rocks under pressure. *Journal of Geophysical Research: Solid Earth*, 85, 925-936.
- 15 KAHRAMAN, S. 2002. The effects of fracture roughness on P-wave velocity. *Engineering Geology*, 63,  
16 347-350.
- 17 KERN, H. 1982. P-and S-wave velocities in crustal and mantle rocks under the simultaneous action of  
18 high confining pressure and high temperature and the effect of the rock microstructure. *High-*  
19 *Pressure Researches in Geoscience*, 15-45.
- 20 KING, M. S., MYER, L. R. & REZOWALLI, J. J. 1986. Experimental studies of elastic-wave propagation in  
21 a columnar-jointed rock mass. *Geophysical prospecting*, 34, 1185-1199.
- 22 KING, M. S., CHAUDRY, N. A. & AHMED, S. Experimental ultrasonic velocities and permeability of  
23 sandstones with aligned cracks. 56th EAEG Meeting, 1994.
- 24 LEE, P. J., LAMBERT, M. F., SIMPSON, A. R., VÍTKOVSKÝ, J. P. & LIGGETT, J. 2006. Experimental  
25 verification of the frequency response method for pipeline leak detection. *Journal of Hydraulic*  
26 *research*, 44, 693-707.
- 27 LI, J. C., LI, H. B., JIAO, Y. Y., LIU, Y. Q., XIA, X. & YU, C. 2014. Analysis for oblique wave propagation  
28 across filled joints based on thin-layer interface model. *Journal of Applied Geophysics*, 102,  
29 39-46.
- 30 LI, J. C. & MA, G. W. 2009. Experimental study of stress wave propagation across a filled rock joint.  
31 *International Journal of Rock Mechanics and Mining Sciences*, 46, 471-478.
- 32 LI, J. C., MA, G. W. & HUANG, X. 2010. Analysis of wave propagation through a filled rock joint. *Rock*  
33 *Mechanics and Rock Engineering*, 43, 789-798.
- 34 LI, J. C., RONG, L., LI, H. & HONG, S. 2018. An SHPB Test Study on Stress Wave Energy Attenuation in  
35 Jointed Rock Masses. *Rock Mechanics and Rock Engineering*, 1-18.
- 36 LI, J. C., WU, W., LI, H. B., ZHU, J. B. & ZHAO, J. 2013. A thin-layer interface model for wave propagation  
37 through filled rock joints. *Journal of Applied Geophysics*, 91, 31-38.
- 38 LIPPARINI, L., TRIPPETTA, F., RUGGIERI, R., BRANDANO, M. & ROMI, A., 2018. Oil distribution in  
39 outcropping carbonate-ramp reservoirs (Maiella Mountain, Central Italy): Three-dimensional  
40 models constrained by dense historical well data and laboratory measurements. *AAPG*  
41 *Bulletin*, 102, 1273-1298.
- 42 LOUATI, M. & GHIDAOUI, M. S. 2017a. High-frequency acoustic wave properties in a water-filled pipe.  
43 Part 1: dispersion and multi-path behaviour. *Journal of Hydraulic Research*, 55, 613-631.
- 44 LOUATI, M. & GHIDAOUI, M. S. 2017b. High-frequency acoustic wave properties in a water-filled pipe.  
45 Part 2: range of propagation. *Journal of Hydraulic Research*, 55, 632-646.
- 46 MA, G. W., LI, J. C. & ZHAO, J. 2011. Three-phase medium model for filled rock joint and interaction  
47 with stress waves. *International journal for numerical and analytical methods in geomechanics*,  
48 35, 97-110.
- 49 MAVKO, G. & JIZBA, D., 1991. Estimating grain-scale fluid effects on velocity dispersion in rocks.  
50 *Geophysics*, 56(12), pp.1940-1949.

- 1 MAVKO, G. & NOLEN-HOEKSEMA, R., 1994. Estimating seismic velocities at ultrasonic frequencies in  
2 partially saturated rocks. *Geophysics*, 59(2), pp.252-258.
- 3 MILLER, S. L. & STEWART, R. R. 1990. Effects of lithology, porosity and shaliness on P-and S-wave  
4 velocities from sonic logs. *Canadian Journal of Exploration Geophysics*, 26, 94-103.
- 5 MONTONE, P. & MARIUCCI, M. T. 2015. P-wave velocity, density, and vertical stress magnitude along  
6 the crustal Po Plain (Northern Italy) from Sonic Log Drilling Data. *Pure and Applied Geophysics*,  
7 172, 1547-1561.
- 8 MORAD, S., AL-AASM, I.S., SIRAT, M. & SATTAR, M.M., 2010. Vein calcite in cretaceous carbonate  
9 reservoirs of Abu Dhabi: Record of origin of fluids and diagenetic conditions. *Journal of*  
10 *Geochemical Exploration*, 106, 156-170.
- 11 MORROW, C., LOCKNER, D., HICKMAN, S., RUSANOV, M. & RÖCKEL, T., 1994. Effects of lithology and  
12 depth on the permeability of core samples from the Kola and KTB drill holes. *Journal of*  
13 *Geophysical Research: Solid Earth*, 99, 7263-7274.
- 14 MÜLLER, T. M., GUREVICH, B. & LEBEDEV, M. 2010. Seismic wave attenuation and dispersion resulting  
15 from wave-induced flow in porous rocks—A review. *Geophysics*, 75, 75A147-75A164.
- 16 NAKAGAWA, S., NIHEI, K.T. & MYER, L.R., 2000. Stop-pass behavior of acoustic waves in a 1D fractured  
17 system. *The Journal of the Acoustical Society of America*, 107(1), pp.40-50.
- 18 NICOLAS, A., FORTIN, J.B., REGNET, J., DIMANOV, A. & GUÉGUEN, Y., 2016. Brittle and semi-brittle  
19 behaviours of a carbonate rock: influence of water and temperature. *Geophysical Journal*  
20 *International*, 206, 438-456.
- 21 PYRAK-NOLTE, L. J., MYER, L. R. & COOK, N. G. W. 1990. Transmission of seismic waves across single  
22 natural fractures. *Journal of Geophysical Research: Solid Earth*, 95, 8617-8638.
- 23 RIENSTRA, S.W. & HIRSCHBERG, A., 2004. An introduction to acoustics. *Eindhoven University of*  
24 *Technology*.
- 25 RISNES, R., MADLAND, M.V., HOLE, M. & KWABIAH, N.K., 2005. Water weakening of chalk—  
26 Mechanical effects of water-glycol mixtures. *Journal of Petroleum Science and Engineering*,  
27 48, 21-36.
- 28 ROKHLIN, S. I. & WANG, Y. J. 1991. Analysis of boundary conditions for elastic wave interaction with  
29 an interface between two solids. *The Journal of the Acoustical Society of America*, 89, 503-  
30 515.
- 31 ROKHLIN, S. I. & HUANG, W. 1992. Ultrasonic wave interaction with a thin anisotropic layer between  
32 two anisotropic solids: Exact and asymptotic-boundary-condition methods. *The Journal of the*  
33 *Acoustical Society of America*, 92, 1729-1742.
- 34 SCHOENBERG, M. 1980. Elastic wave behavior across linear slip interfaces. *The Journal of the*  
35 *Acoustical Society of America*, 68, 1516-1521.
- 36 SINHA, U.N., SINGH, B., 2000. Testing of rock joints filled with gouge using a triaxial apparatus.  
37 *International Journal of Rock Mechanics and Mining Sciences*, 37, 963-981.
- 38 STEIN, S. & WYSESSION, M. 2009. *An introduction to seismology, earthquakes, and earth structure*,  
39 John Wiley & Sons.
- 40 TANIMOTO, C. & KISHIDA, K., 1994. Seismic geotomography: Amplitude versus velocity in  
41 consideration of joint aperture and spacing. In *1st North American Rock Mechanics*  
42 *Symposium*. American Rock Mechanics Association.
- 43 TOKSÖZ, M. N., JOHNSTON, D. H. & TIMUR, A. 1979. Attenuation of seismic waves in dry and saturated  
44 rocks: I. Laboratory measurements. *Geophysics*, 44, 681-690.
- 45 TRIPPETTA, F., COLLETTINI, C., VINCIGUERRA, S. & MEREDITH, P.G., 2010. Laboratory measurements  
46 of the physical properties of Triassic Evaporites from Central Italy and correlation with  
47 geophysical data. *Tectonophysics*, 492, 121-132.
- 48 TRIPPETTA, F. & GEREMIA, D., 2019. The seismic signature of heavy oil on carbonate reservoir through  
49 laboratory experiments and AVA modelling. *Journal of Petroleum Science and Engineering*  
50 WOOD, A.B., 1949. A textbook of sound: London, G. Bell and Sons, Ltd, pp.361-362.

- 1 WU, W., LI, J. C. & ZHAO, J. 2014. Role of filling materials in a P-wave interaction with a rock fracture.  
2 *Engineering Geology*, 172, 77-84.
- 3 WU, W. & ZHAO, J. 2015. Effect of water content on P-wave attenuation across a rock fracture filled  
4 with granular materials. *Rock Mechanics and Rock Engineering*, 48, 867-871.
- 5 WYLIE, E. B., STREETER, V. L. & SUO, L. 1993. *Fluid transients in systems*, Prentice Hall Englewood Cliffs,  
6 NJ.
- 7 XU, P.C. & PARRA, J.O., 2003. Effects of single vertical fluid-filled fractures on full waveform dipole  
8 sonic logs. *Geophysics*, 68(2), 487-496.
- 9 YANG, Z.Y., LO, S.C. & DI, C.C., 2001. Reassessing the joint roughness coefficient (JRC) estimation using  
10 Z 2. *Rock mechanics and rock engineering*, 34(3), pp.243-251.
- 11 ZHAO, J. & CAI, J. G. 2001. Transmission of elastic P-waves across single fractures with a nonlinear  
12 normal deformational behavior. *Rock Mechanics and Rock Engineering*, 34, 3-22.
- 13 ZHAO, J., CAI, J. G., ZHAO, X. B. & LI, H. B. 2006a. Experimental study of ultrasonic wave attenuation  
14 across parallel fractures. *Geomechanics and Geoengineering: An International Journal*, 1, 87-  
15 103.
- 16 ZHAO, J., ZHAO, X. B. & CAI, J. G. 2006b. A further study of P-wave attenuation across parallel fractures  
17 with linear deformational behaviour. *International Journal of Rock Mechanics and Mining*  
18 *Sciences*, 43, 776-788.
- 19 ZHAO, X., ZHAO, J. & CAI, J. G. 2006. P-wave transmission across fractures with nonlinear  
20 deformational behaviour. *International journal for numerical and analytical methods in*  
21 *geomechanics*, 30, 1097-1112.
- 22 ZHU, J. B., PERINO, A., ZHAO, G. F., BARLA, G., LI, J. C., MA, G. W. & ZHAO, J. 2011. Seismic response  
23 of a single and a set of filled joints of viscoelastic deformational behaviour. *Geophysical*  
24 *Journal International*, 186, 1315-1330.
- 25 ZHU, J. B., ZHAO, X. B., WU, W. & ZHAO, J. 2012. Wave propagation across rock joints filled with  
26 viscoelastic medium using modified recursive method. *Journal of Applied Geophysics*, 86, 82-  
27 87.
- 28 ZHU, J. B. & ZHAO, J. 2013. Obliquely incident wave propagation across rock joints with virtual wave  
29 source method. *Journal of Applied Geophysics*, 88, 23-30.
- 30 ZHU, J. B., ZHAO, X. B., LI, J. C., ZHAO, G. F. & ZHAO, J. 2011. Normally incident wave propagation  
31 across a joint set with the virtual wave source method. *Journal of Applied Geophysics*, 73, 283-  
32 288.
- 33 ZHU, J. B., ZHAO, X. B., WU, W. & ZHAO, J. 2012. Wave propagation across rock joints filled with  
34 viscoelastic medium using modified recursive method. *Journal of Applied Geophysics*, 86, 82-  
35 87.

# 1 List of symbols:

$S_i, S_j$	Number of samples
$V_{P1}, V_{P2}$	Wave velocities of the jointed rock samples for P-waves at different central frequencies
$SD_{P1}, SD_{P2}$	Standard deviations of wave velocities in jointed rock samples for different P-waves
$V_{P\_intact}, V_P$	Wave velocities of the intact and jointed rock samples, respectively
DRV	Decrease rate of wave velocity through jointed rock samples
$V_{WP1}, V_{WP2}$	Wave velocities in fluid-filled rock joints for P-waves at different central frequencies
$SD_{WP1}, SD_{WP2}$	Standard deviations of wave in fluid-filled rock joints for different P-waves
$H$	Joint thickness
$L$	Total length of the natural jointed rock sample/reference intact rock
$t$	Measured arrival time of the transmitted pulse
$t_0$	Travel time of the pulse through the rock sample with a dry closed jointed
$T_{ct}, T_{cf}$	Wave transmission coefficient in the time domain and frequency domain, respectively
$A_{1\_max}(t), A_{2\_max}(t)$	Maximum voltages of received initial signals through the intact and jointed rock samples, respectively
$A_{1\_max}(f), A_{2\_max}(f)$	Maximum spectral amplitudes of tapered initial waves across the intact and the jointed samples, respectively
$Q, Q_1, Q_2$	Attenuation quality factor
$SD_{Q1}, SD_{Q2}$	Standard deviations of $Q$ of jointed rock samples for different P-waves
$c, c_1, c_2$	Phase wave velocity
$f, f_1, f_2$	Wave frequency
$x$	Wave travel length
$G(x), G_1(x), G_2(x)$	Geometrical factor
$W_c$	Water content in the joint



1

Table 1. Physical and mechanical properties of rock samples

No. of sample	UCS (MPa)	$E$ (GPa)	$\nu$	$M_{dry}$ (g)	$M_{wet}$ (g)	Density (kg/m <sup>3</sup> )	Porosity (%)	P-wave velocity (km/s)	
								$f_1 = 0.1$ MHz	$f_2 = 1$ MHz
$S_I$	138.86	58.80	0.24	498.72	500.08	2.637	0.719	$5.048 \pm 0.082$	$5.220 \pm 0.007$
$S_J$	--	--	--	500.65	501.75	2.692	0.576	$4.943 \pm 0.015$	$5.117 \pm 0.027$

\*Note: P-wave velocities of samples were measured under the fully-saturated situation.  $S_I$  and  $S_J$  refer to intact rock sample and jointed rock sample, respectively.

UCS is uniaxial compressive strength;  $E$  is Elastic modulus;  $\nu$  is the Poisson's ratio;  $M_{dry}$  is the dry mass of rock sample; and  $M_{wet}$  is the wet mass of rock sample.

4

Table 2. The average values and standard deviations of wave velocities in rock samples with a single fluid-filled joint

	$W_c = 25\%$				$W_c = 50\%$				$W_c = 75\%$				$W_c = 100\%$			
	$V_{P1}$ (km/s)	$SD_{P1}$	$V_{P2}$ (km/s)	$SD_{P2}$	$V_{P1}$ (km/s)	$SD_{P1}$	$V_{P2}$ (km/s)	$SD_{P2}$	$V_{P1}$ (km/s)	$SD_{P1}$	$V_{P2}$ (km/s)	$SD_{P2}$	$V_{P1}$ (km/s)	$SD_{P1}$	$V_{P2}$ (km/s)	$SD_{P2}$
$H=2$ mm	4.940	0.027	5.139	0.038	5.012	0.035	5.166	0.040	5.031	0.023	5.176	0.036	5.052	0.065	5.206	0.033
$H=4$ mm	4.716	0.058	4.892	0.024	4.794	0.041	4.924	0.042	4.797	0.037	4.939	0.034	4.819	0.045	4.968	0.034
$H=6$ mm	4.551	0.014	4.689	0.037	4.591	0.027	4.717	0.031	4.607	0.031	4.734	0.039	4.639	0.042	4.767	0.038
$H=8$ mm	4.372	0.020	4.521	0.039	4.424	0.030	4.541	0.027	4.458	0.024	4.547	0.025	4.471	0.041	4.581	0.040
$H=10$ mm	4.218	0.028	4.355	0.021	4.266	0.023	4.382	0.023	4.291	0.027	4.386	0.023	4.316	0.037	4.427	0.021
$H=12$ mm	4.079	0.013	4.210	0.030	4.120	0.021	4.228	0.032	4.142	0.023	4.242	0.025	4.175	0.034	4.284	0.019
$H=14$ mm	3.970	0.022	4.075	0.019	4.002	0.022	4.087	0.023	4.035	0.021	4.103	0.035	4.046	0.035	4.143	0.016

\*Note:  $H$  is joint thickness and  $W_c$  is water content in the joint;  $V_{P1}$  and  $V_{P2}$  are wave velocities of the jointed rock samples for P-waves at 0.1 MHz and 1 MHz, respectively;  $SD_{P1}$  and  $SD_{P2}$  are standard deviations of wave velocities in the jointed rock samples for P-waves at 0.1 MHz and 1 MHz, respectively.



Table 3. The average values and standard deviations of wave velocities in different fluid-filled rock joints

	$W_c = 25\%$				$W_c = 50\%$				$W_c = 75\%$				$W_c = 100\%$			
	$V_{WP1}$ (km/s)	$SD_{WP1}$	$V_{WP2}$ (km/s)	$SD_{WP2}$	$V_{WP1}$ (km/s)	$SD_{WP1}$	$V_{WP2}$ (km/s)	$SD_{WP2}$	$V_{WP1}$ (km/s)	$SD_{WP1}$	$V_{WP2}$ (km/s)	$SD_{WP2}$	$V_{WP1}$ (km/s)	$SD_{WP1}$	$V_{WP2}$ (km/s)	$SD_{WP2}$
$H=2$ mm	0.980	0.059	1.200	0.077	1.129	0.102	1.270	0.085	1.178	0.094	1.308	0.080	1.250	0.158	1.404	0.078
$H=4$ mm	1.174	0.055	1.304	0.039	1.284	0.081	1.358	0.065	1.290	0.075	1.395	0.053	1.330	0.076	1.442	0.049
$H=6$ mm	1.274	0.024	1.354	0.042	1.329	0.046	1.397	0.035	1.352	0.048	1.414	0.037	1.402	0.053	1.472	0.047
$H=8$ mm	1.324	0.026	1.400	0.039	1.370	0.039	1.421	0.022	1.415	0.036	1.424	0.009	1.433	0.049	1.485	0.049
$H=10$ mm	1.348	0.044	1.412	0.019	1.387	0.034	1.431	0.022	1.416	0.026	1.440	0.021	1.446	0.040	1.501	0.022
$H=12$ mm	1.355	0.016	1.421	0.028	1.393	0.03	1.440	0.027	1.417	0.025	1.451	0.025	1.454	0.031	1.503	0.017
$H=14$ mm	1.387	0.029	1.428	0.017	1.412	0.032	1.443	0.022	1.446	0.016	1.453	0.029	1.457	0.029	1.500	0.017

\*Note:  $H$  is joint thickness and  $W_c$  is water content in the joint;  $V_{WP1}$  and  $V_{WP2}$  are wave velocities of the jointed rock samples for P-waves at 0.1 MHz and 1 MHz, respectively;  $SD_{WP1}$  and  $SD_{WP2}$  are standard deviations of wave velocities in single fluid-filled rock joint for P-waves at 0.1 MHz and 1 MHz, respectively.

Table 4. The standard deviations of attenuation quality factor  $Q$  for different fluid-filled rock joints

	$W_c = 25\%$		$W_c = 50\%$		$W_c = 75\%$		$W_c = 100\%$	
	$SD_{Q1}$	$SD_{Q2}$	$SD_{Q1}$	$SD_{Q2}$	$SD_{Q1}$	$SD_{Q2}$	$SD_{Q1}$	$SD_{Q2}$
$H = 2$ mm	0.300	0.626	0.187	0.150	0.275	0.286	0.268	0.326
$H = 4$ mm	0.378	0.177	0.373	0.241	0.175	0.260	0.071	0.371
$H = 6$ mm	0.161	0.452	0.127	0.368	0.357	0.324	0.121	0.591
$H = 8$ mm	0.351	0.258	0.196	0.364	0.142	0.259	0.197	0.576
$H = 10$ mm	0.281	0.160	0.168	0.296	0.178	0.238	0.132	0.644
$H = 12$ mm	0.383	0.174	0.161	0.551	0.205	0.292	0.171	0.538
$H = 14$ mm	0.037	0.223	0.361	0.263	0.334	0.342	0.302	0.210

\*Note:  $H$  is joint thickness and  $W_c$  is water content in the joint;  $SD_{Q1}$  and  $SD_{Q2}$  are standard deviations of attenuation quality factor  $Q$  for different fluid-filled rock joints for P-waves at 0.1 MHz and 1 MHz, respectively.

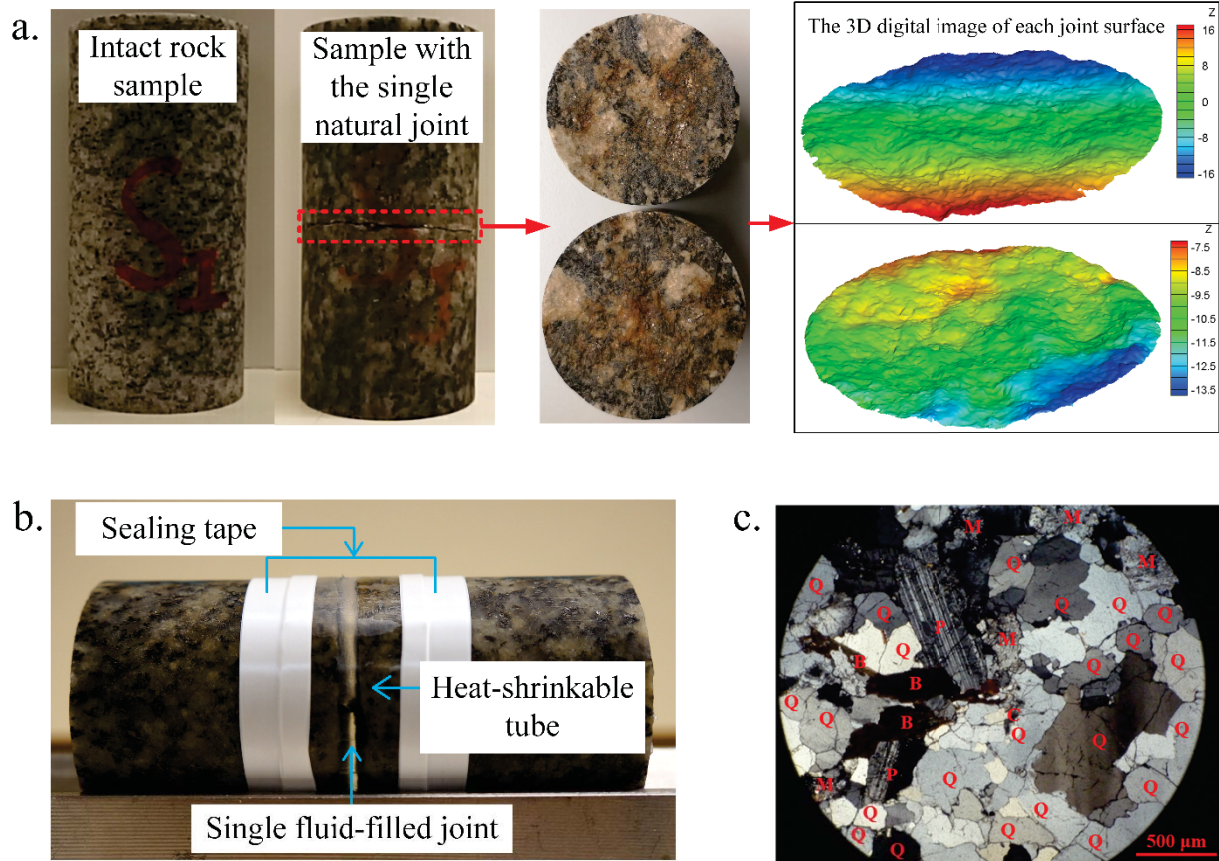


Figure 1. Information of rock material used in this study: a. The intact rock sample, the jointed rock sample and the 3D digital image of its joint surfaces; b. rock sample with an artificially joint filled with fluid; c. the representative optical microscope image (Q: Quartz, P: Plagioclase, M: Microcline, B: Biotite, C: Chlorite).

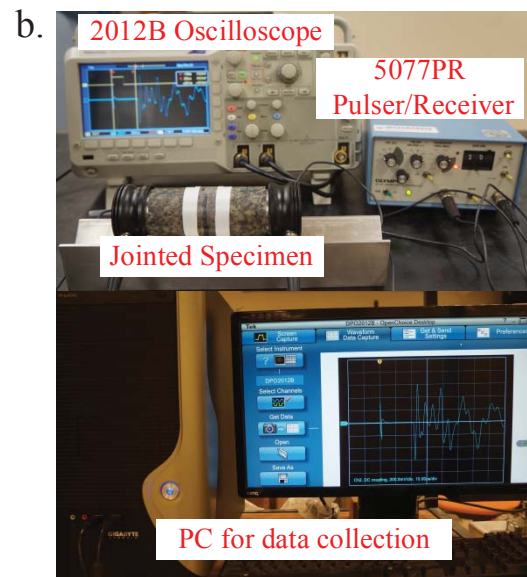
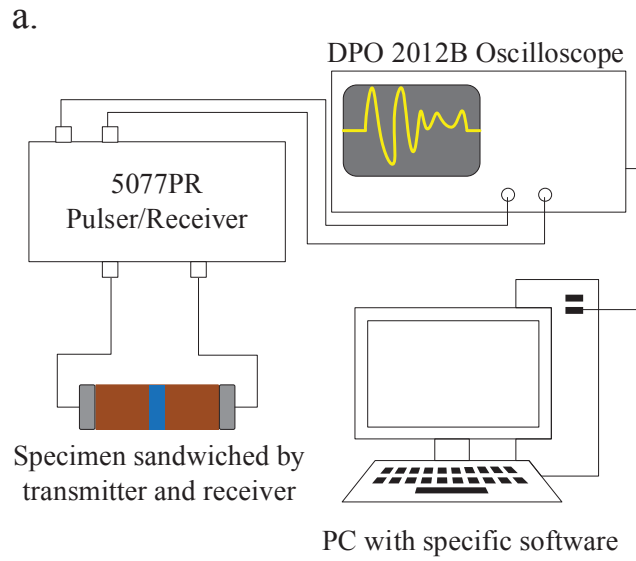


Figure 2. The ultrasonic testing system: a. The schematic of experimental set-up; and b. the apparatuses and sample in the laboratory.

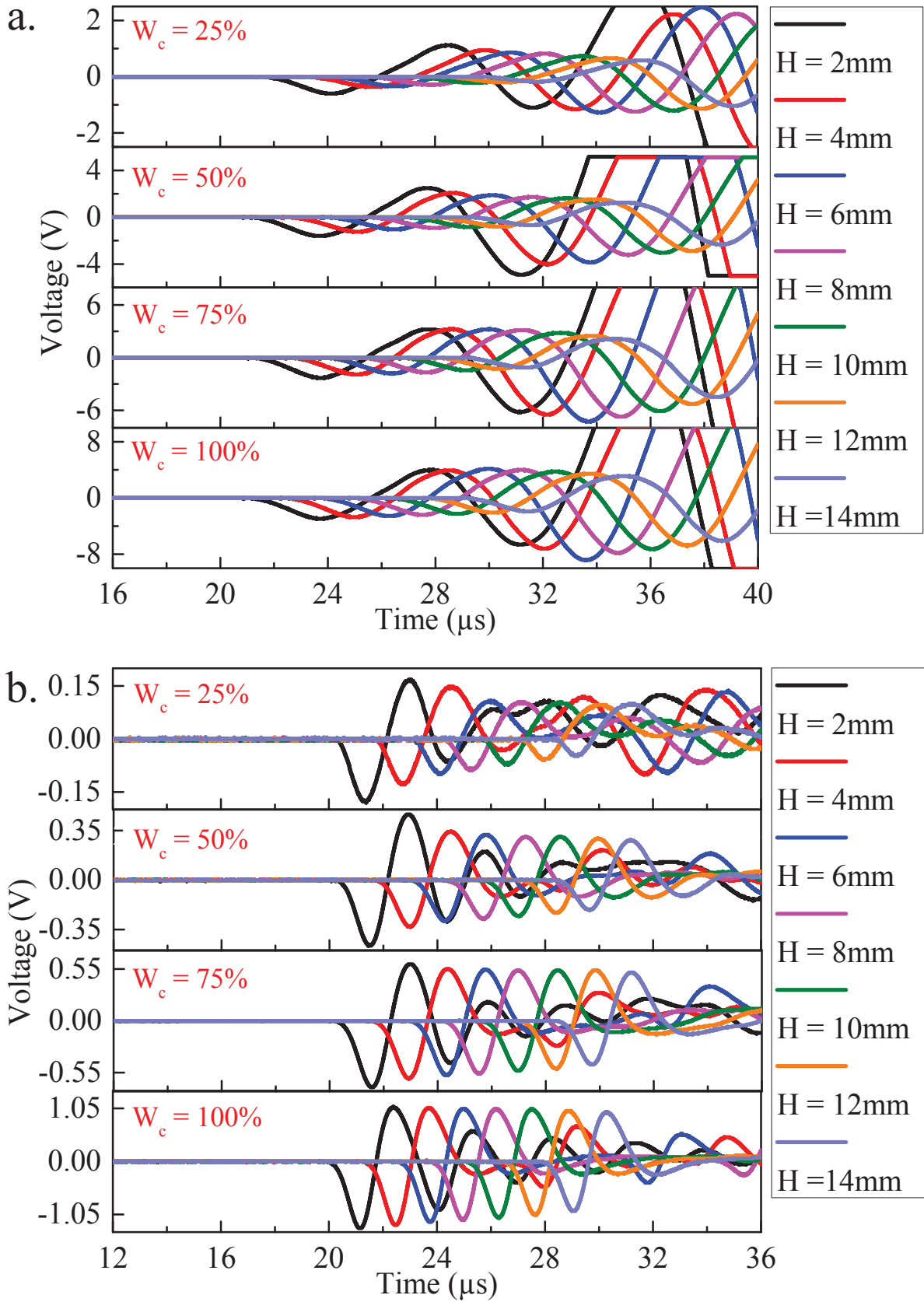


Figure 3. Measured transmitted waveforms through rock samples with a single fluid-filled joint: a. Received waveforms from P-wave transducer of 0.1 MHz; b. received waveforms from P-wave transducer of 1 MHz.

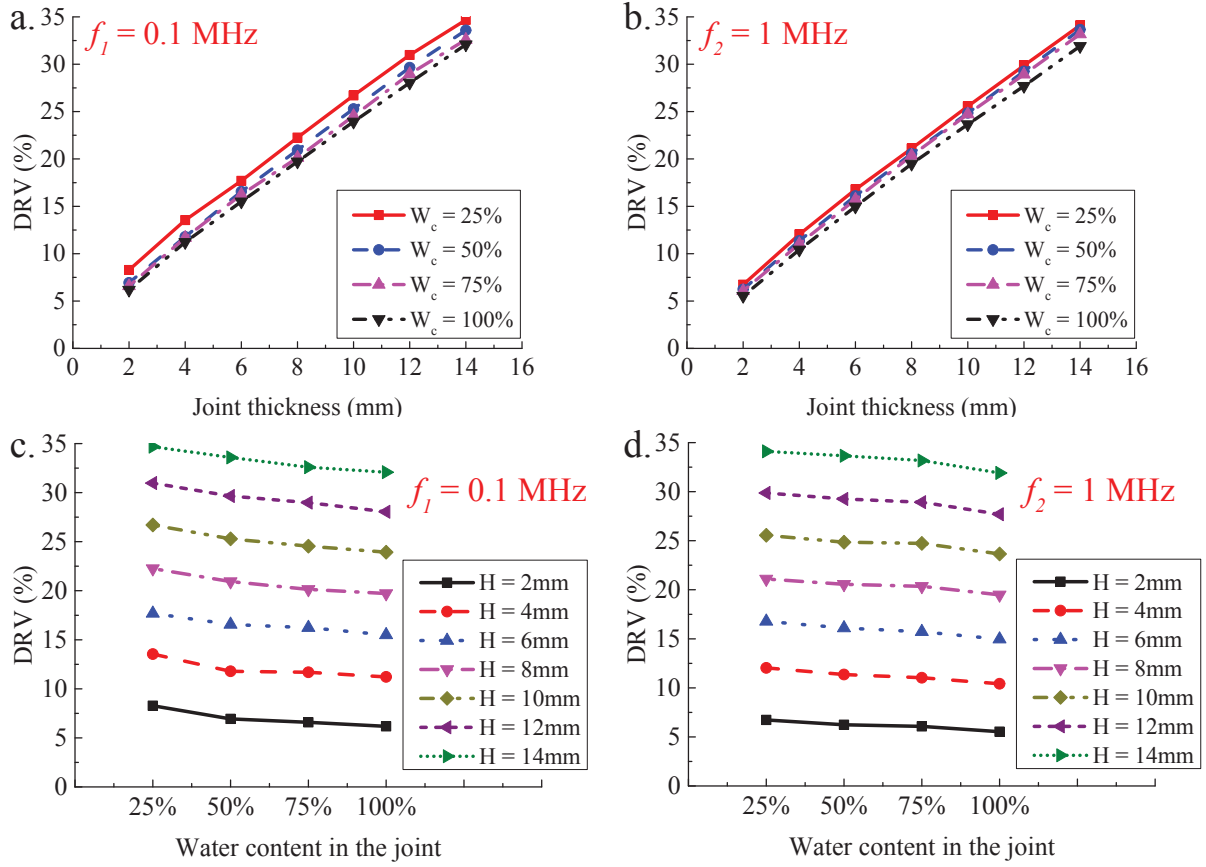


Figure 4. The DRV for ultrasonic wave propagation across a single fluid-filled rock joint: a. DRV vs joint thickness for different water contents in joint where the frequency of the ultrasonic transducer is 0.1 MHz; b. DRV vs joint thickness for different water contents in joint where the frequency of the ultrasonic transducer is 1 MHz; c. DRV vs water content in joint for different joint thickness where the frequency of the ultrasonic transducer is 0.1 MHz; d. DRV vs water content in joint for different joint thickness where the frequency of the ultrasonic transducer is 1 MHz.

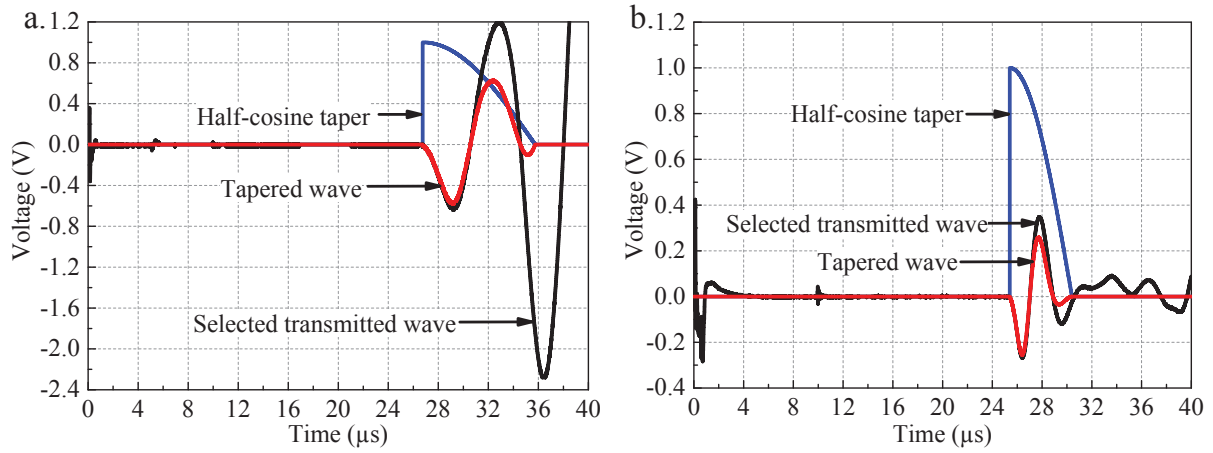
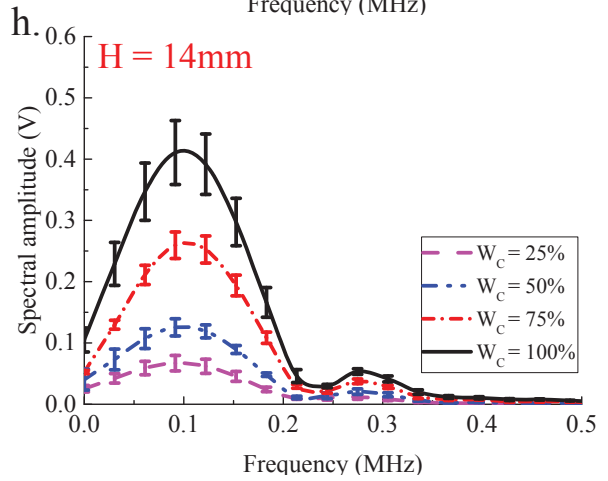
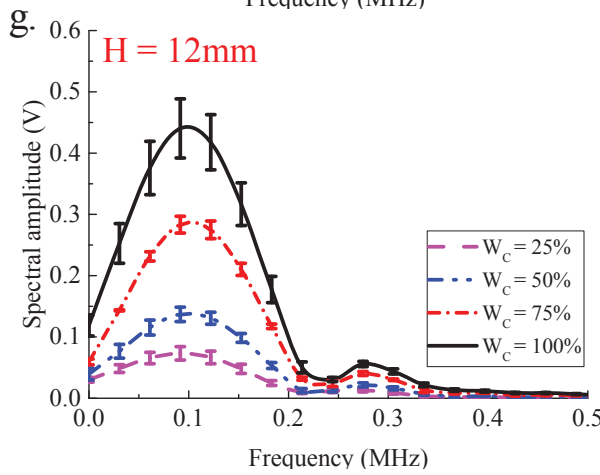
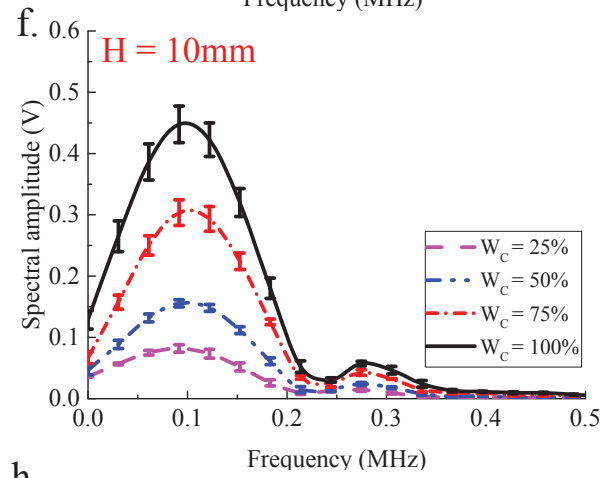
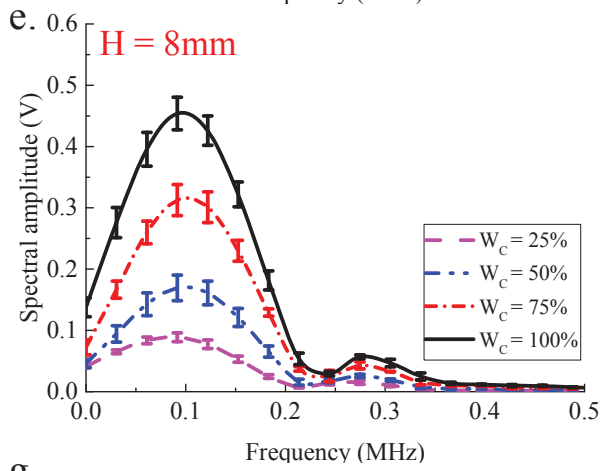
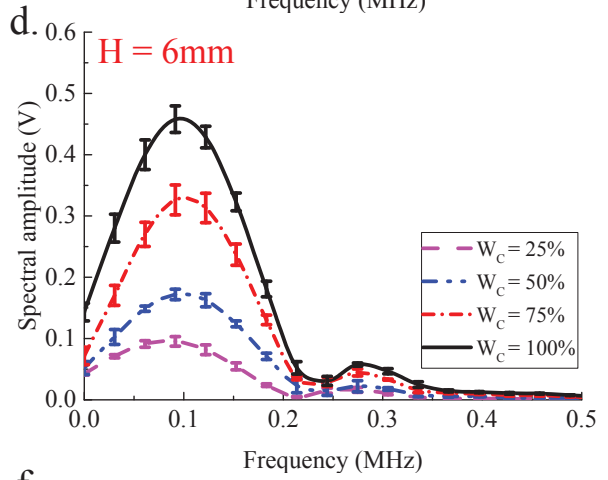
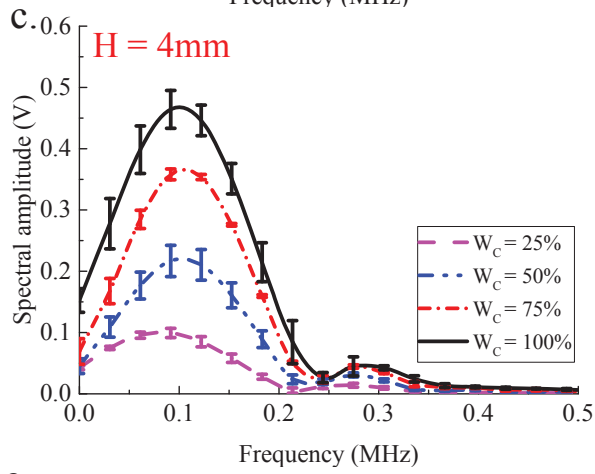
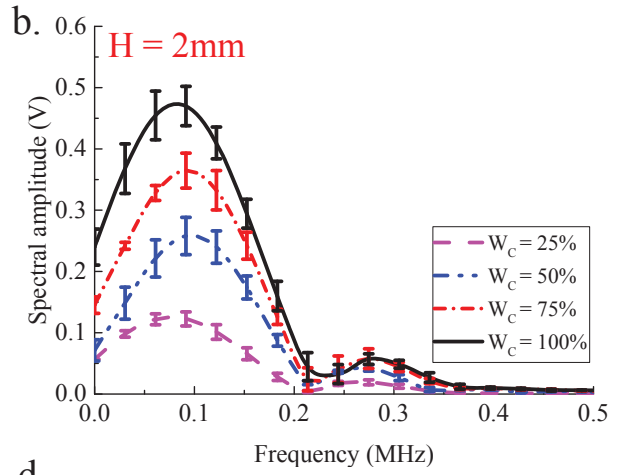
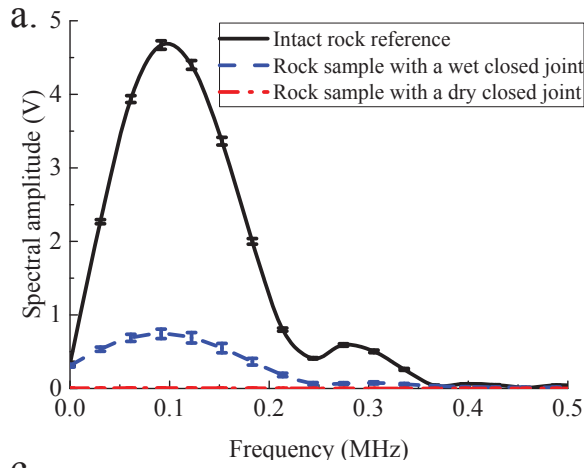


Figure 5. Tapers applied to received signals, original transmitted waves and tapered waves for wave transmission across rock samples with a single fluid-filled joint: a. Half-cosine taper with 9- $\mu\text{s}$  window for P-waves with a frequency of 0.1 MHz; b. half-cosine taper with 5- $\mu\text{s}$  window for P-waves with a frequency of 1 MHz.





1 Figure 6. Spectra amplitudes of tapered transmitted pulses through rock samples with a single fluid-  
2 filled rock joint for incident P-waves with a central frequency of 0.1 MHz: a. Reference intact rock  
3 sample and rock sample with a closed joint; b.  $H = 2$  mm; c.  $H = 4$  mm; d.  $H = 6$  mm; e.  $H = 8$  mm; f.  
4  $H = 10$  mm; g.  $H = 12$  mm; h.  $H = 14$  mm.

5

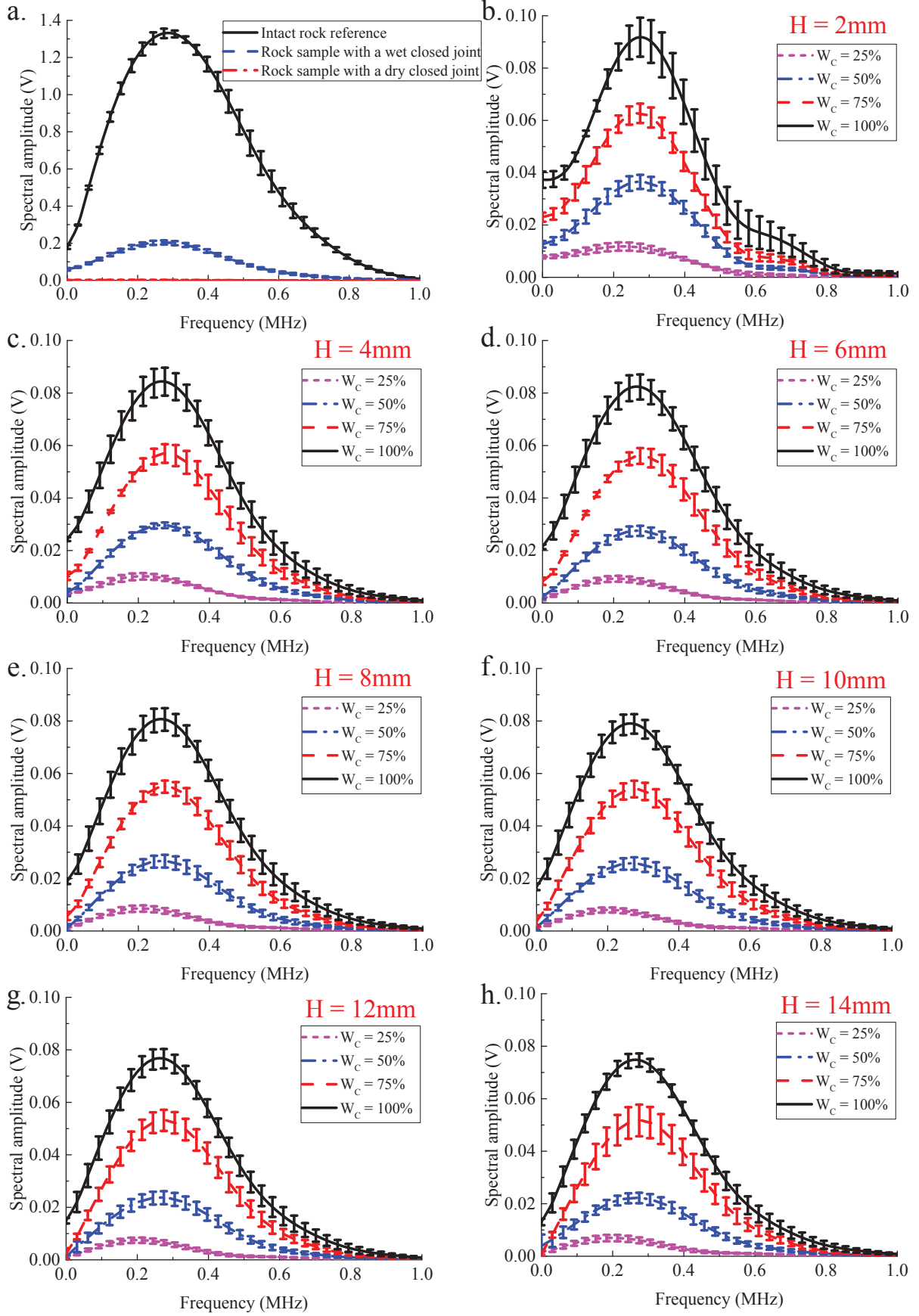


Figure 7. Spectral amplitudes of tapered initial transmitted pulses through different rock samples for incident P-waves with a central frequency of 1 MHz: a. Reference intact rock sample and rock sample

- 1 with a closed joint; b.  $H = 2\text{mm}$ ; c.  $H = 4\text{mm}$ ; d.  $H = 6\text{mm}$ ; e.  $H = 8\text{mm}$ ; f.  $H = 10\text{mm}$ ; g.  $H = 12\text{mm}$ ;
- 2 h.  $H = 14\text{mm}$ .
- 3

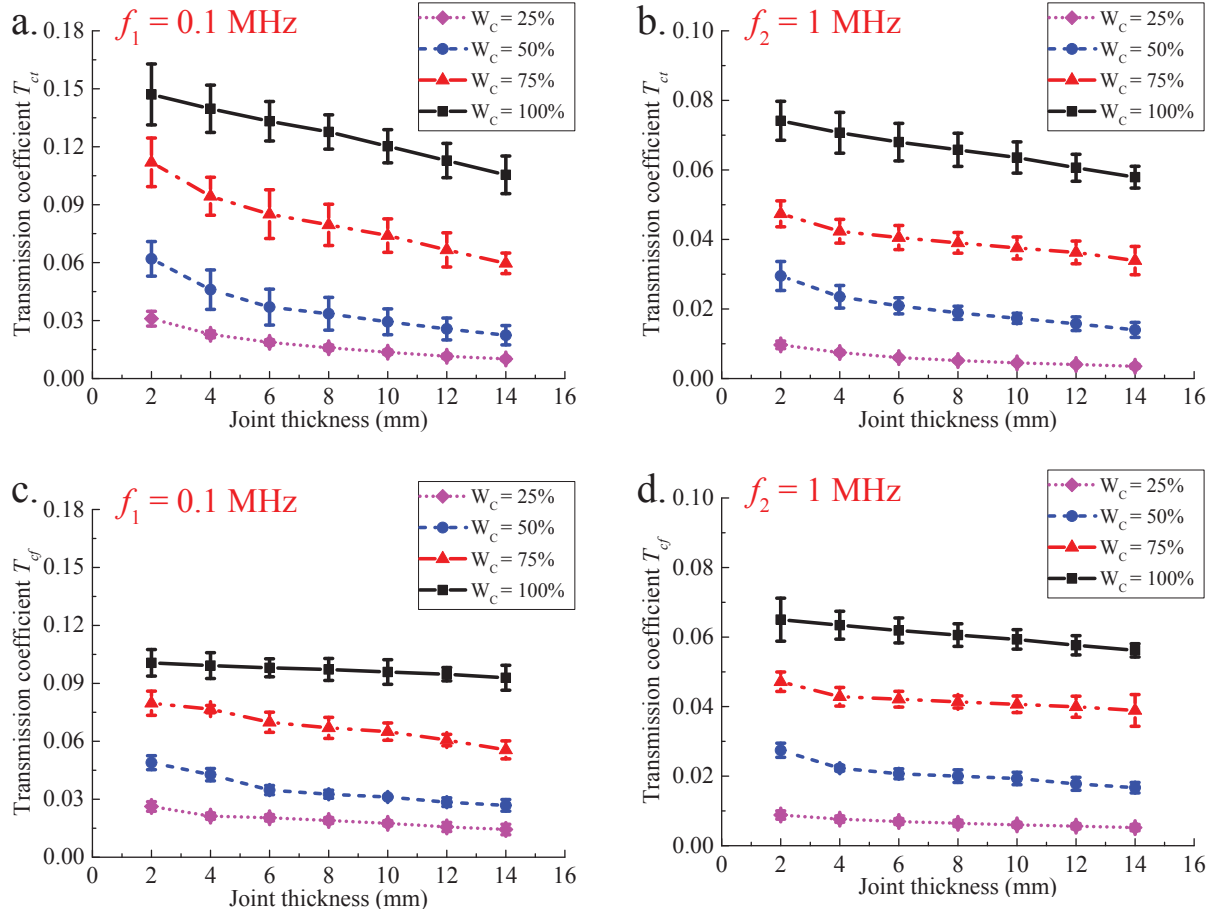


Figure 8. Transmission coefficients for ultrasonic P-wave transmission across a single fluid-filled rock joint: a. Transmission coefficient in time domain vs joint thickness where the wave frequency is 0.1 MHz; b. transmission coefficient in time domain vs joint thickness where the wave frequency is 1 MHz; c. transmission coefficient in frequency domain vs joint thickness where the wave frequency is 0.1 MHz; d. transmission coefficient in frequency domain vs joint thickness where the wave frequency is 1 MHz.

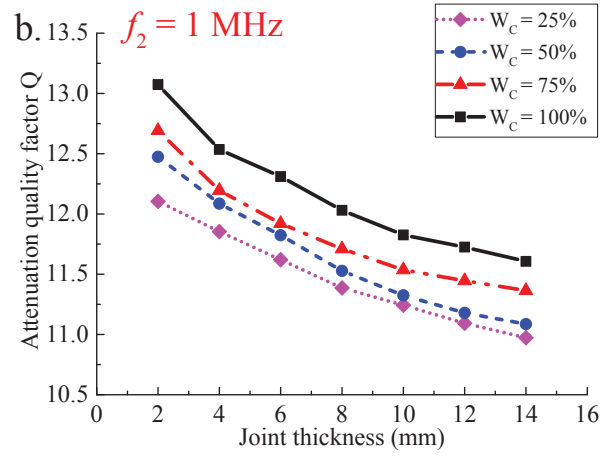
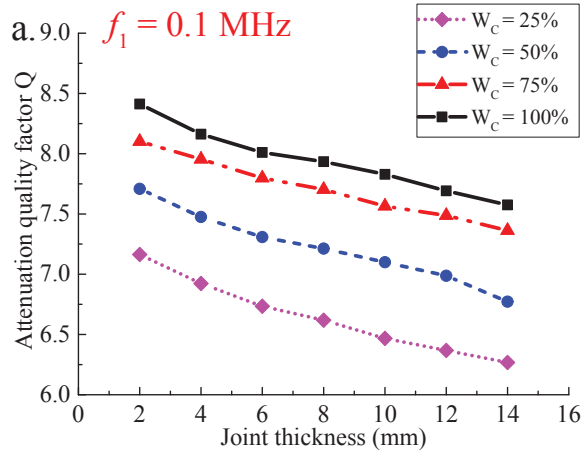


Figure 9. The average values of  $Q$  as a function of joint thickness for different water contents in joint:  
a. P-wave with a frequency of 0.1 MHz; b. P-wave with a frequency of 1 MHz.

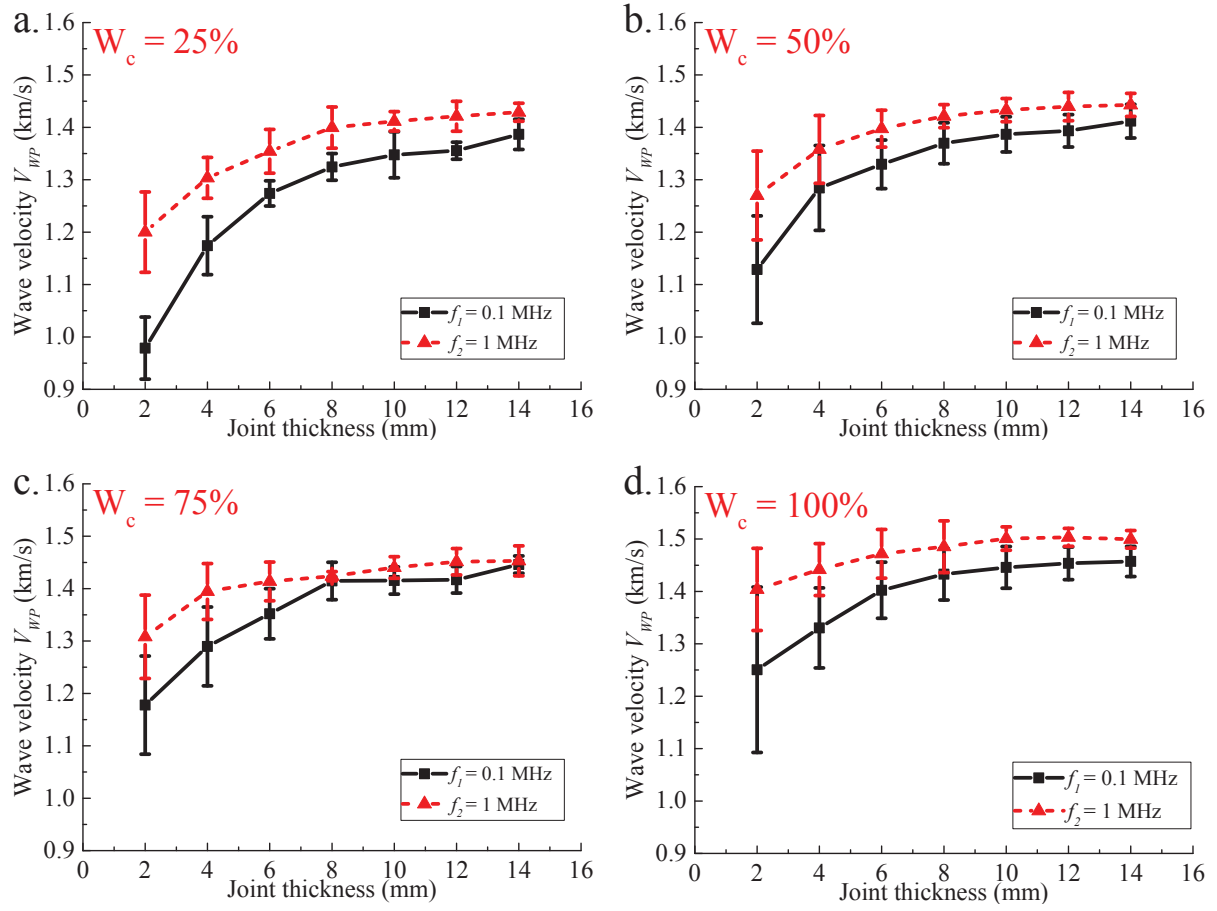


Figure 10. Wave velocity vs joint thickness at different wave frequencies for wave propagation across fluid-filled rock joints with different water contents: a.  $W_c = 25\%$ ; b.  $W_c = 50\%$ ; c.  $W_c = 75\%$ ; d.  $W_c = 100\%$ .